0022-5347/03/1693-0881/0
THE JOURNAL OF UROLOGY®

Vol. 169, 881–885, March 2003
Printed in U.S.A.
DOI: 10.1097/01.ju.0000046367.49923.c6

STONE RETROPULSION DURING HOLMIUM:YAG LITHOTRIPSY

HO LEE, R. TRES RYAN, JOEL M. H. TEICHMAN, JEEHYUN KIM, BERNARD CHOI, NAVANIT V. ARAKERI AND A. J. WELCH

From the Division of Urology, University of Texas Health Science Center, San Antonio and Departments of Mechanical Engineering, Electrical and Computer Engineering, and Biomedical Engineering, University of Texas, Austin, Texas

ABSTRACT

Purpose: We modeled retropulsion during holmium:YAG lithotripsy on the conservation of momentum, whereby the force of ejected fragment debris off of the calculous surface should equal the force of retropulsion displacing the stone. We tested the hypothesis that retropulsion occurs as a result of ejected stone debris.

Materials and Methods: Uniform calculous phantoms were irradiated with holmium:YAG energy in air and in water. Optical fiber diameter and pulse energy were varied. Motion of the phantom was monitored with high speed video imaging. Laser induced crater volume and geometry were characterized by optical coherence tomography. To determine the direction of plume laser burn paper was irradiated at various incident angles.

Results: Retropulsion was greater for phantoms irradiated in air versus water. Retropulsion increased as fiber diameter increased and as pulse energy increased ($p < 0.001$). Crater volumes increased as pulse energy increased ($p < 0.05$) and generally increased as fiber diameter increased. Crater geometry was wide and shallow for larger fibers, and narrow and deeper for smaller fibers. The ejected plume propagated in the direction normal to the burn paper surface regardless of the laser incident angle.

Conclusions: Retropulsion increases as pulse energy and optical fiber diameter increase. Vector analysis of the ejected plume and crater geometry explains increased retropulsion using larger optical fibers. Holmium:YAG lithotripsy should be performed with small optical fibers to limit retropulsion.

KEY WORDS: ureter; ureteral calculi; lithotripsy, laser; movement

The long laser pulse duration of holmium:YAG lithotripsy (250 microseconds) produces a pear-shaped vapor bubble that collapses asymmetrically.[1] Collapse of the asymmetrical vapor bubble causes weak pressure waves of less than 8 bars with no cavitation or shock wave effects.[2,3] Although the pressure waves of holmium:YAG lithotripsy are less than those of other lithotripsy modalities, some retropulsion occurs.[4] Retropulsion forces the urologist to move the optical fiber and ureteroscope to the new calculous position, which may add operative time and inconvenience. In lasers with a short pulse duration of less than 1 microsecond retropulsion occurs mainly due to strong pressure waves or laser induced shock waves caused by symmetrical collapse of a spherical cavitation bubble.[5,6] If this phenomena occurred in holmium:YAG lithotripsy, retropulsion would be greatest for small diameter fibers due to high fluence.[7] Moreover, higher pulse energy would produce greater retropulsion. Experimentally holmium:YAG lithotripsy causes a different retropulsion pattern. Larger fibers produce greater retropulsion than smaller fibers, while higher pulse energy results in greater retropulsion than lower pulse energy.[4] Since retropulsion represents displacement, we modeled retropulsion on the conservation of momentum, whereby the force of ejected fragment debris off of the calculous surface would equal the force of retropulsion displacing the stone in the opposite direction. In this study we tested the hypothesis that retropulsion occurs as a result of ejected stone debris.

MATERIALS AND METHODS

Uniform calculous phantoms were prepared using plaster of Paris. Phantoms had a mass of 150 mg. and volume of 125 mm.[3] The calculous phantom was placed in an in vitro ureteral model consisting of a clear glass tube with an inner diameter of 12.5 mm. (fig. 1). The tube was filled with air or deionized water. A clinical and a scientific holmium:YAG laser were used in our study. Each laser emits 2.1 μm. laser pulses with a pulse duration of 250 microseconds. Holmium:YAG energy was delivered to a calculous phantom in contact mode with low OH^- quartz fibers 272, 365, 550 and 940 μm. in diameter (SlimLine 200, 365, 550 and 1000 fibers) (Lumenis, Santa Clara, California), respectively. Before each irradiation the irradiation spot (tracer beam) was adjusted with a 3-axis translation stage, so that it was centered on the phantom. Before and after ablation laser energy out of the distal end of the fiber was measured with an energy meter equipped with a pyroelectric joulemeter.

Calculous phantom motion was monitored with a high speed video camera that enabled us to obtain images at 1,000 frames per second. A white light source was used to illuminate the glass tube and phantom. The high speed video camera and lens system were adjusted to capture the motion of the phantom with a spatial resolution of 3 μm. At least 10 measurements were made per condition. Acquired images were transferred to a personal computer equipped with a frame grabber. Edges of the transferred digital images were enhanced using computer software.

A series of experiments was done under various conditions to measure initial phantom displacement after the pulse. We varied pulse energy (200 to 1,000 mJ.) and fiber diameter (272, 365, 550 and 940 μm.). For irradiation in air the phantom was displaced away from the fiber. However, for irradiation in water at an energy level of 800 and 1,000 mJ. using the 272, 365 and 550 μm. fibers the laser pulse caused the phantom to move away initially. The phantom rocked back

Accepted for publication October 18, 2002.

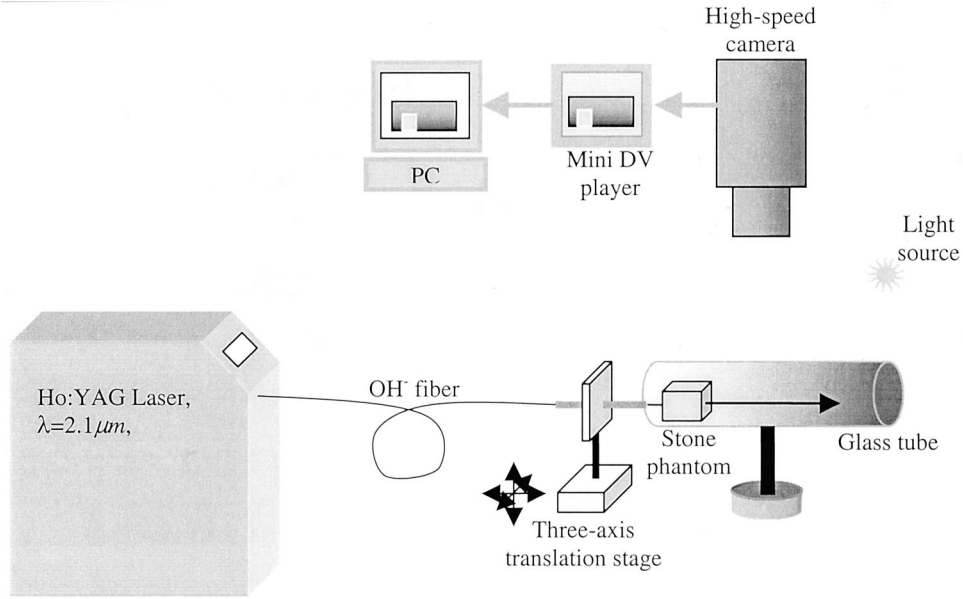

FIG. 1. Experimental setup to measure initial stone velocity after pulse. *PC*, personal computer. *DV*, digital video

toward the fiber and then continued to move away from the fiber. Thus, we report displacement in water only for 200 and 500 mJ. Retropulsive force was assumed as an impact due to the short time frame of less than 1 millisecond. Initial displacement (displacement during the first millisecond after the onset of the laser pulse) of the recoiling phantom was measured by observing the first 2 frames after the laser pulse. Initial velocity of the phantom was calculated from initial displacement and travel time (1 millisecond). Linear recoil momentum was determined using the equation, RM = mV, where RM represents linear recoil momentum in kg. × m. per second, m represents the phantom mass in kg. and V represents initial velocity in m. per second.

Laser induced craters were examined with an optical coherence tomography system to determine ablation crater shape quantitatively. A series of cross-sectional crater images was obtained over the whole crater. Ablation volume was determined from optical coherence tomography images over the crater volume.

The propagation direction of the laser induced ablation plume governs the direction and amount of the recoil momentum. To investigate how the plume propagates after being ablated we used the high speed video camera to monitor the dynamics of the laser induced plume. Laser burn paper was placed 2 cm. away from the fiber at different angles with respect to the fiber (perpendicular and ± 45 degrees) and irradiated in air with a single holmium:YAG laser pulse using a 940 μm. fiber and 500 mJ. pulse energy. The trajectory of the ejected ablation plume was determined from the acquired image sequences.

RESULTS

When phantoms were irradiated in air or water, displacement increased as fiber diameter increased and as pulse energy increased (tables 1 and 2). The corresponding recoil momenta increased linearly as pulse energy increased for all fiber sizes ($p < 0.001$, figs. 2 and 3). For a given laser energy recoil momentum increased with fiber diameter ($p < 0.001$).

Figure 4 shows laser induced, crater optical coherence tomography cross-sectional profiles after irradiation with a single holmium:YAG laser pulse. An increase in pulse energy produced larger craters for all 4 fibers. Crater shape was also affected by fiber size. At a given pulse energy irradiation with the larger fiber produced wider and shallower craters compared with a smaller fiber. Figure 5 shows ablation volume calculated from a cross-sectional optical coherence tomography image of a crater. Ablation volumes of the 940 μm fiber at pulse energies of 200 and 400 mJ. were smaller than those of the other 3 fibers at the same energy levels. In each other case the fiber with the larger diameter ablated about 25% more than the fiber with the smaller diameter. The ejected plume propagated in the direction normal to the burn paper surface regardless of the incident angle of the laser (fig. 6).

DISCUSSION

Calculous retropulsion increases as pulse energy increases.[4] This result was expected because higher energies caused larger ablation volumes that increased phantom recoil momentum. The linear relationship of ablation volume to input laser energy during photothermal lithotripsy implies that the amount of stone ablation affects stone recoil. The enhanced momentum of phantom recoil irradiated in air compared with water underscores that retropulsion during holmium:YAG lithotripsy depends primarily on recoil of ejected fragments. If cavitation bubbles caused retropulsion during holmium:YAG lithotripsy, displacement would not occur for irradiation in air. In contrast, during photo-acoustic lithotripsy re-

TABLE 1. *Stone displacement in air*

Fiber Diameter (μm.)	Mean Displacement ± SD (μm.)				p Value*
	200 mJ.	400 mJ.	600 mJ.	800 mJ.	
272	120 ± 38	183 ± 32	232 ± 42	318 ± 50	<0.001
365	133 ± 35	247 ± 27	296 ± 18	363 ± 32	<0.0001
550	165 ± 29	288 ± 38	387 ± 54	470 ± 22	<0.0001
940	160 ± 48	364 ± 96	684 ± 67	854 ± 86	<0.0001
p Value	0.03	<0.0001	<0.0001	<0.0001	

* Pairwise comparisons of fiber diameters were significant at 200 mJ. for 272 versus 550 and 272 versus 940 μm., at 400 mJ. for all fiber comparisons except 365 versus 550 μm., at 600 mJ. for all fiber comparisons and at 800 mJ. for all comparisons except 272 versus 365 μm., and pairwise comparisons of energy cohorts were significant for all 272, 365, 550 and 940 μm. fiber comparisons.

TABLE 2. *Stone displacement in water*

Fiber Diameter (μm.)	Mean Displacement ± SD (μm.)*		p Value†
	200 mJ.	500 mJ.	
272	51 ± 11	84 ± 17	<0.001
365	82 ± 23	120 ± 30	<0.001
550	172 ± 28	206 ± 32	0.002
940	172 ± 54	358 ± 136	<0.001

* p <0.001.

† Pairwise differences were statistically significant at 200 mJ. for 272 versus 550, 272 versus 940, 365 versus 550 and 365 versus 940 μm. fibers, and at 500 mJ. for 272 versus 550, 272 versus 940, 365 versus 550, 365 versus 940 and 550 versus 940 μm. fibers.

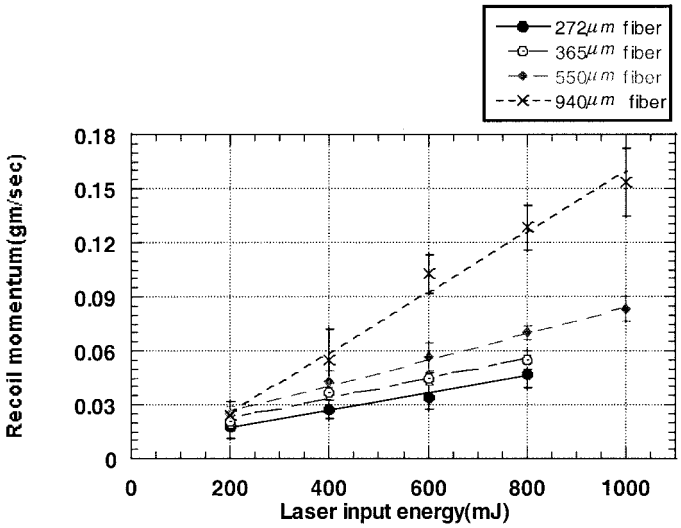

FIG. 2. Mean recoil momentum of calculous phantoms as function of holmium:YAG laser energy for different size fibers in air. Error bars indicate SD.

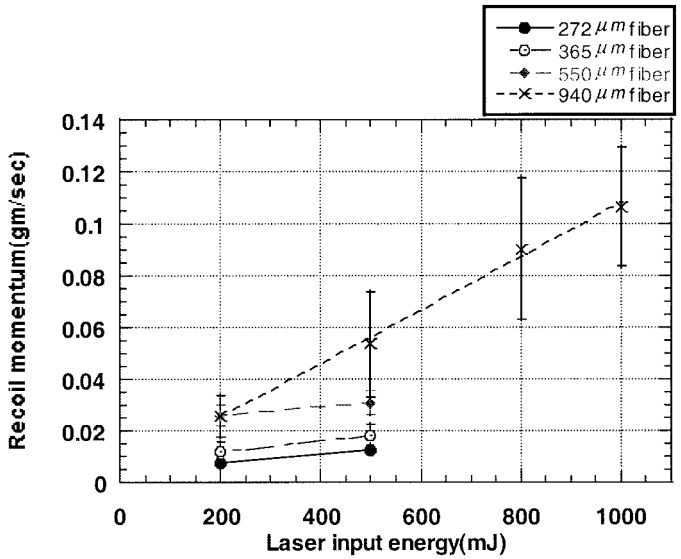

FIG. 3. Calculous recoil momentum as function of holmium:YAG laser energy for different size fibers in water.

coil depends more on the size of the cavitation bubble than on debris.[4]

However, recoil cannot be explained simply by the mass of ejected fragments. To compare the recoil momentum of different fibers we assessed several parameters, including the laser induced pressure wave, initial velocity of the ejected particle, total mass removal and propagation direction of the

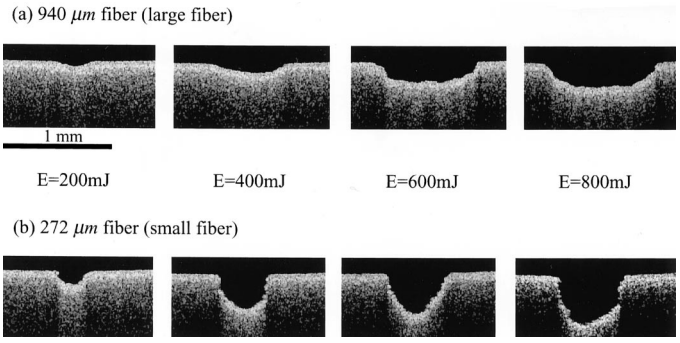

FIG. 4. Representative cross-sectional optical coherence tomography images of laser crater created using 940 (*a*) and 272 (*b*) μm. fibers. Smaller fiber produced narrow, deep craters compared with larger fiber.

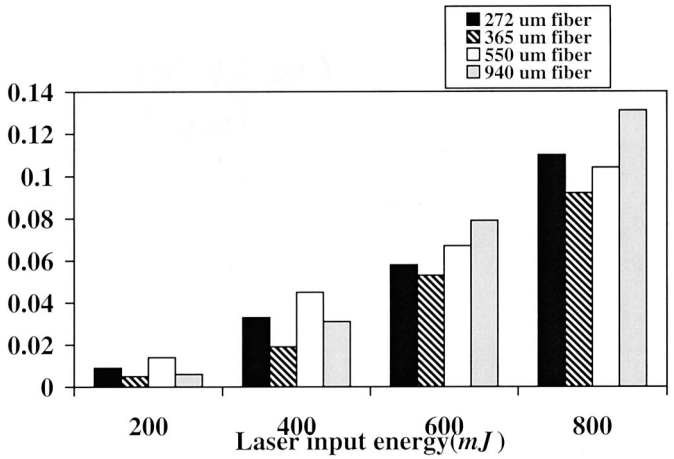

FIG. 5. Mean ablation volume as function of laser energy. Comparisons of energy levels were statistically significant for each fiber (p <0.05). Comparisons of fiber diameters were statistically significant for 200 mJ. pulse energy for 272 versus 365, 365 versus 550 and 550 versus 940 μm. fibers, for 400 mJ. for all fibers except 272 versus 940 and 550 versus 940 μm., for 600 mJ. for 272 versus 365, 272 versus 550 and 550 versus 940 μm. fibers, and for 800 mJ. except for 272 versus 550 μm. fibers (p <0.05).

ejected particle. At any given input energy the smaller fiber produced a higher ejected particle pressure wave and velocity than a larger fiber as a result of a higher fluence and temperature increase within the irradiated volume. Accordingly the enhanced recoil of larger fibers seems paradoxical.

Increased retropulsion with larger fibers resulted from crater geometry. On optical coherence tomography crater width increased and crater depth decreased as fiber diameter increased. Figure 7 shows how the differences in crater topography could affect recoil. We assumed that the laser produced 5 fragments that were about to eject from the surface. Propagation velocity and the mass of all particles were assumed to be the same for simplicity. Since laser induced fragments eject in a direction normal to the surface (fig. 6), fragments would generate an equal force on the remainder of the calculus in the opposite direction of displacement. To analyze force terms we divided the force vector into 2 directions (x and y axes). The opposing x components of particles canceled each other. Only y components produced calculous recoil and recoil momentum should correspond to the sum of y components. Accordingly by comparing the total y components of the 2 craters we could determine which crater would produce a higher recoil momentum.

Fragments 1 and 5 had only x components. The y components of fragment 3 in the 2 cases were identical. However, for fragments 2 and 4 the y components varied based on

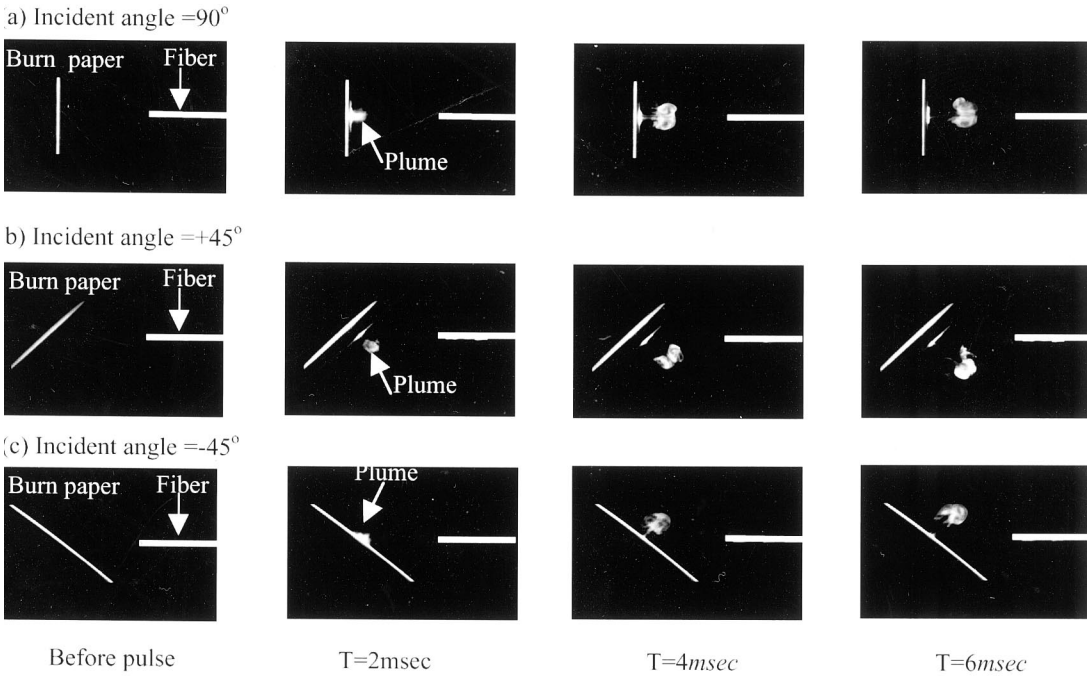

FIG. 6. Plume displacement as function of incident angle. Regardless of incident angle between laser beam (fiber axis) and burn paper plume orientation was always at normal incidence to burn paper. *T*, time.

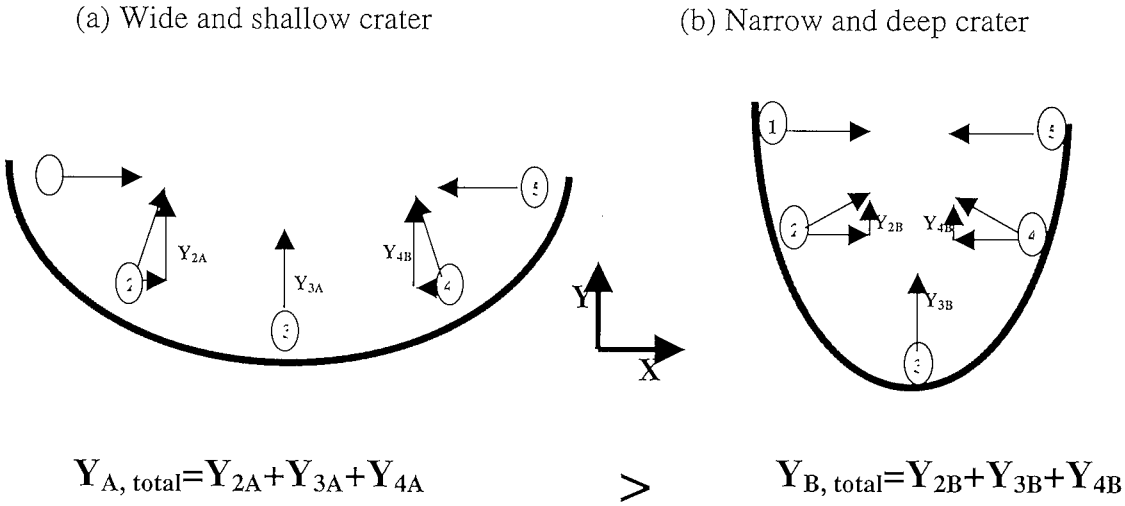

FIG. 7. Ejection of ablated particles from 2 distinct craters

crater geometry. Fragments 2 and 4 of case 1 had a larger y component than those of case 2. As a result, recoil momentum was higher for case 1 than case 2.

Clinically a larger optical fiber produces a wide and shallow crater as well as greater stone recoil than a smaller fiber. Thus, smaller fibers may be more desirable for clinical lithotripsy. Another possibility would be to ablate stones at the periphery of the calculus to minimize retropulsion. However, this alternate strategy would result in less efficient lithotripsy because photothermal lithotripsy is most efficient at a normal laser incidence.[8] In fact, with the fiber oriented to the extreme periphery of the stone surface (that is a tangential orientation but still in contact) a large vapor bubble is produced but no lithotripsy occurs.[4]

An interesting phenomenon was that the calculus rocked to and fro after the laser pulse, possibly due to microjet dynamics. During lithotripsy the surrounding water absorbs holmium:YAG energy efficiently. The water is vaporized and forms a bubble. The expanding bubble reaches maximal expansion and subsequently collapses. If a solid boundary exists near the bubble, the bubble collapses asymmetrically due to retarded flow near the solid boundary.[9, 10] We assume that this phenomena may be responsible for the difference in maximal and net displacement results reported by White et al.[4] In their study net displacement was less than maximal displacement, implying initial retropulsion followed by recoil back toward the fiber. However, our experiment was done with single pulse energy to examine the effects of contact lithotripsy and minimize the effects of the vapor bubble. In the experiment of White et al in which the laser was run as a train of pulses there was undoubtedly a separation distance between the optical fiber and stone surface after initial ablation. As a result, other dynamics may have been factors in stone displacement, such as vapor bubble expansion and collapse with corresponding pressure waves and reentrant water flow dynamics. Thus, in clinical lithotripsy the optical

fiber may not always be in contact with the stone surface as the train of laser pulses is delivered. Without the constant contact between fiber tip and stone surface to limit vapor expansion a larger vapor bubble may be produced, which in turn produces larger pressure transients as high as 20 bars with a pulse energy of 1.5 J.[4] Although these pressure transients are still too low to fragment stones, they may add some additional momentum to retropulsion, particularly for small fragments. Lithotripsy proceeds most efficiently in contact mode to maximize fragmentation and minimize pressure transients.

Crater volumes in the current study were consistent with previously reported data on holmium:YAG lithotripsy.[11] In that study holmium:YAG craters across multiple calculous compositions were narrow and deep for smaller fibers, and wide and shallow for larger fibers. Moreover, crater volume increased with increased pulse energy. Interestingly the current data show that larger fibers may produce larger volume ablation craters than smaller fibers, which is a finding at odds with our own earlier data on lithotripsy efficiency.[4] In the previous study a 365 μm. fiber was more efficient than other fibers based on fluence and fiber durability considerations. A possible explanation for this apparent discrepancy is the different methodologies. In the previous series we ablated calcium oxalate monohydrate calculi with up to 1 kJ. irradiation, which produced fiber damage with correspondingly less efficient beam profiles. In the current study we assessed single pulse ablation craters using polished fibers to minimize any confounding factors.

CONCLUSIONS

Retropulsion occurs as a result of fragment ejection from the stone surface. Retropulsion increases as the laser energy and the fiber diameter increases. Crater geometry is a major factor in recoil momentum that explains why larger fibers produce increased retropulsion. Crater volume is another factor in recoil momentum that explains why increased pulse energy results in increased retropulsion. To minimize retropulsion during holmium:YAG lithotripsy we suggest using small diameter fibers at modest energy levels.

REFERENCES

1. Jensen, E. D., Asshauer, T., Frenz, M., Motamedi, M., Delacretaz, G. and Welch, A. J.: Effect of pulse duration on bubble formation and laser-induced pressure waves during holmium laser ablation. Lasers Surg Med, **18:** 278, 1996
2. Chan, K. F., Welch, A. J., Teichman, J. M. H. and McGuff, H. S.: Acoustic transients during holmium:YAG lithotripsy. J Endourol, suppl., **13:** A22, abstract, 1999
3. Vassar, G. J., Chan, K. F., Teichman, J. M., Glickman, R. D., Weintraub, S. T., Chan, K. F. et al: Holmium:YAG lithotripsy: photothermal mechanism. J Endourol, **13:** 181, 1999
4. White, M. D., Moran, M. E., Calvano, C. J., Borhan-Manesh, A. and Mehlhaff, B. A.: Evaluation of retropulsion caused by holmium:YAG laser with various power settings and fibers. J Endourol, **12:** 183, 1998
5. Rink, K., Delacretaz, G. and Salathe, R. P.: Fragmentation process of current laser lithotripters. Lasers Surg Med, **16:** 134, 1995
6. Kuznetsov, L. I.: Recoil momentum at a solid surface during developed laser ablation. Quantum Electron, **23:** 1191, 1993
7. Vassar, G. J., Teichman, J. M. H. and Glickman, R. D.: Holmium: YAG lithotripsy efficiency varies with energy density. J Urol, **160:** 471, 1998
8. Teichman, J. M. H., Rao, R. D., Glickman, R. D. and Harris, J. M.: Holmium:YAG lithotripsy: the laser incident angle matters. J Urol, **159:** 690, 1998
9. Plesset, M. S. and Chapman, R. B.: Collapse of an initially spherical vapor cavity in the neighborhood of a solid boundary. J Fluid Mechanics, **47:** 283, 1971
10. Lauterborn, W. and Bolle, H.: Experimental investigations of cavitation bubble collapse in the neighborhood of a solid boundary. J Fluid Mechanics, **72:** 391, 1975
11. Teichman, J. M. H., Vassar, G. J. and Glickman, R. D.: Holmium: yttrium-aluminum-garnet lithotripsy efficiency varies with stone composition. Urology, **52:** 392, 1998